Electronic Supplementary Material (ESI) for Journal of Materials Chemistry A.
This journal is © The Royal Society of Chemistry 2021

Electronic Supplementary Information

Incomplete amorphous phosphorization on the surface of crystalline cobalt molybdate to accelerate hydrogen evolution

Jin Qian,[ab] Shanlin Li,[b] Qian Liu,[b] Ruguang Ma,*[bc] Shengjuan Li,*[a] and Jiacheng Wang* [bd]

[a.] School of Materials Science and Engineering, University of Shanghai for Science and Technology, 516 Jungong Road, Shanghai 200093, P. R. China

[b.] State Key Laboratory of High Performance Ceramics and Superfine Microstructure, Shanghai Institute of Ceramics, Chinese Academy of Sciences, 1295 Dingxi Road, Shanghai 200050, P. R. China

[c.] School of Materials Science and Engineering, Suzhou University of Science and Technology, 99 Xuefu Road Suzhou, 215011, China.

[d.] University of Chinese Academy of Sciences, 19A Yuquan Rd, Shijingshan District, 100049 Beijing, P. R. China

Corresponding authors.

E-mail addresses: maruguang@mail.sic.ac.cn (R. Ma); usstshenli@usst.edu.cn (S. Li); jiacheng.wang@mail.sic.ac.cn (J. Wang).

Synthesis of single-phase cobalt phosphide (CoP_x) on nickel foam (NF)

The cobalt carbonate hydroxide (CoCH) precursor was synthesized by using a method reported by Huang et al.[1] Firstly, 2 mmol $Co(NO_3)_2 \cdot 6H_2O$ and 10 mmol urea were dissolved in 35 mL of deionized water, and stirred violently for 0.5 h. And then, the above pink solution was transferred into a Teflon lined stainless-steel autoclave with 50 mL capacity, where a piece of pretreated Ni foam (2×3 cm^2) was immersed and allowed to stand against the wall, After wards, the autoclave was sealed and maintained at 120 °C for 6h and left to cool down to room temperature naturally. Finally, the CoCH precursor was washed with deionized water and absolute ethanol several times and finally dried at 60 °C for overnight. To obtain the single-phase CoP_x, the as-prepared precursor was annealed in Ar atmosphere in the presence of $NaH_2PO_2 \cdot H_2O$ (0.3 g) as the phosphorus source at 300 °C with the ramping rate of 2 $°C \cdot min^{-1}$ and kept for 2 h.

Preparation of Pt/C on NF

40 wt.% Pt/C (5 mg) was dispersed into 2 mL mixed solution containing 0.48 mL water, 0.02 mL 5% Nafion solution, and 0.5 mL ethanol. The solution was then ultrasonically treated for 30 minutes to form a uniform catalyst ink (2.5 $mg \cdot mL^{-1}$). Then, 0.05 mL catalyst ink was loaded on the NF electrode with the surface area of 1.0 cm^2 for four times, and dried at room temperature for 24 h. Consequently, the loading mass of Pt/C was around 0.5 $mg \cdot cm^{-2}$.

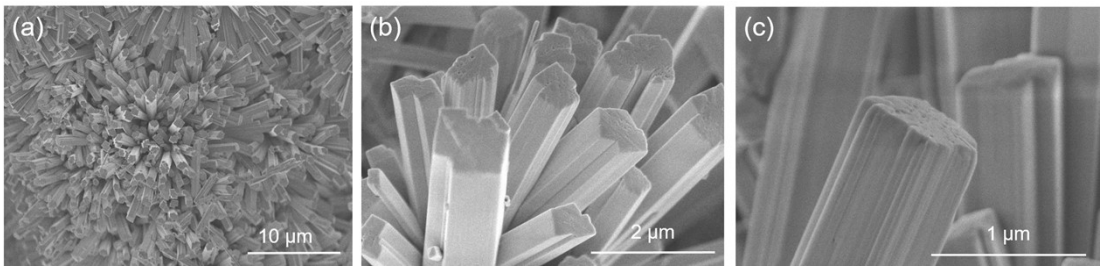

Fig. S1 Low and high-magnifications SEM images of $CoMoO_4$.

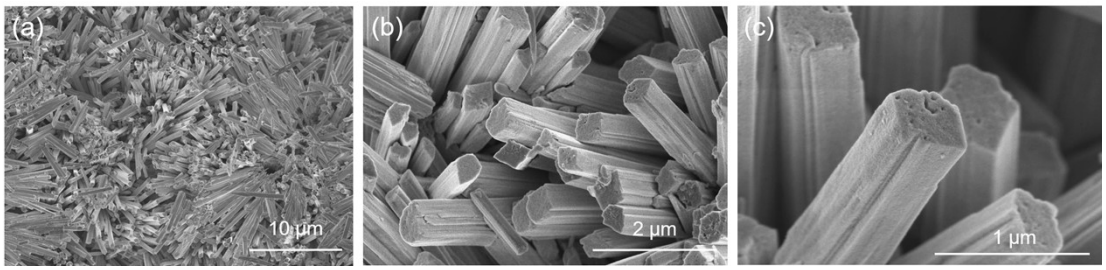

Fig. S2 Low and high-magnifications SEM images of $CoMoO_4$@a-CoP_x.

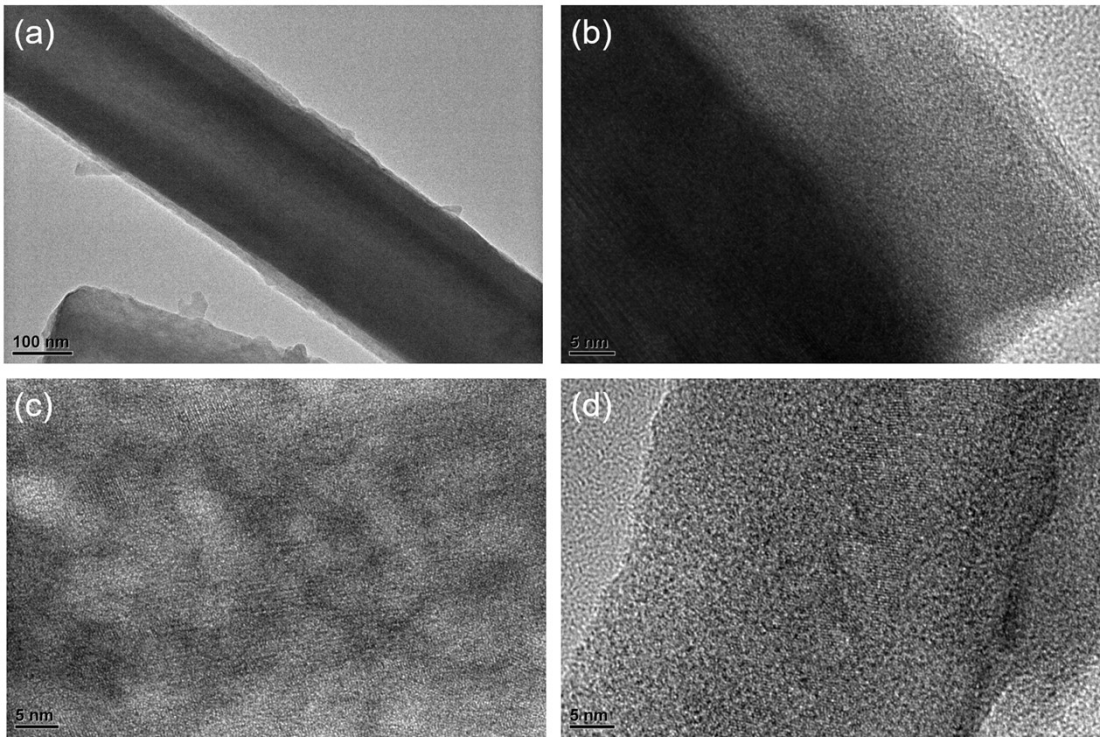

Fig. S3 Low and high-magnifications TEM images of $CoMoO_4$@a-CoP_x.

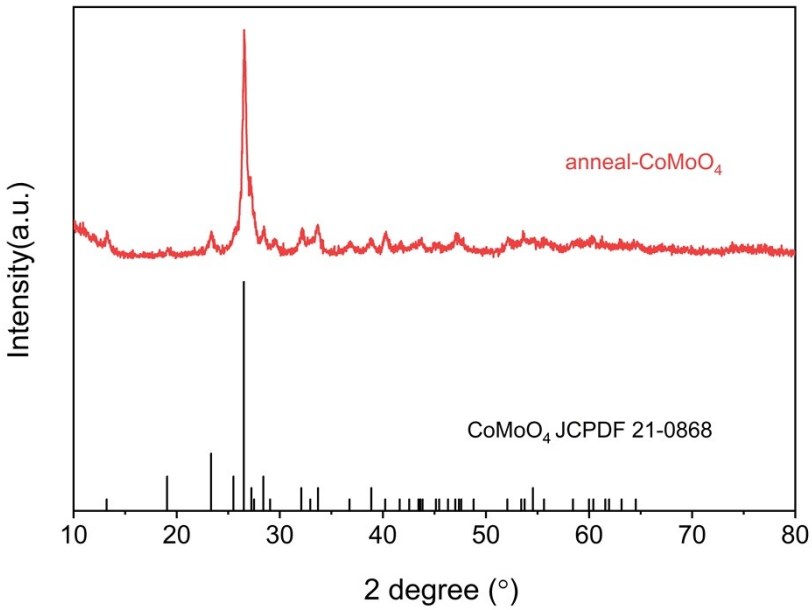

Fig. S4 XRD pattern of $CoMoO_4$ annealed at 300°C.

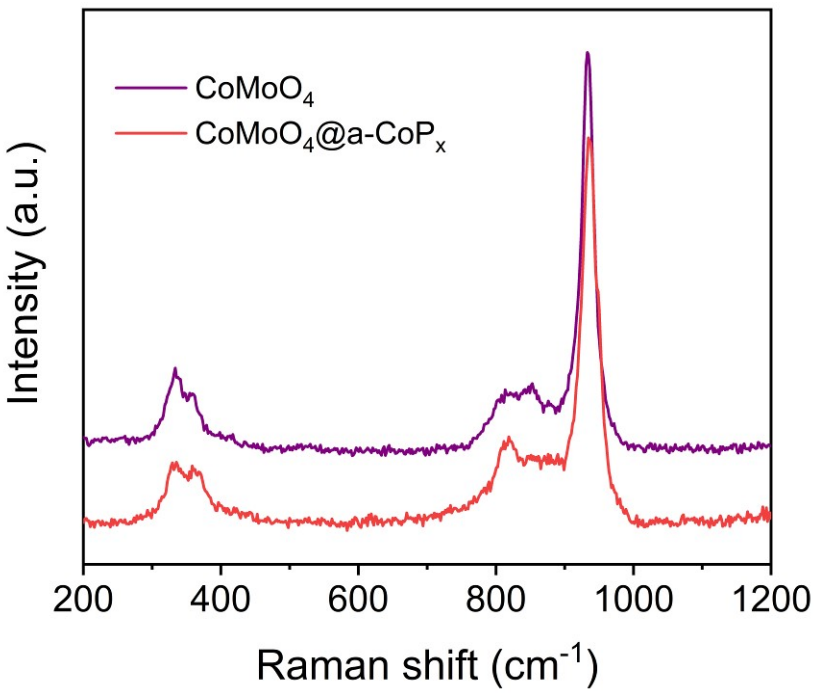

Fig. S5 Raman spectra of $CoMoO_4$ and $CoMoO_4$@a-CoP_x samples

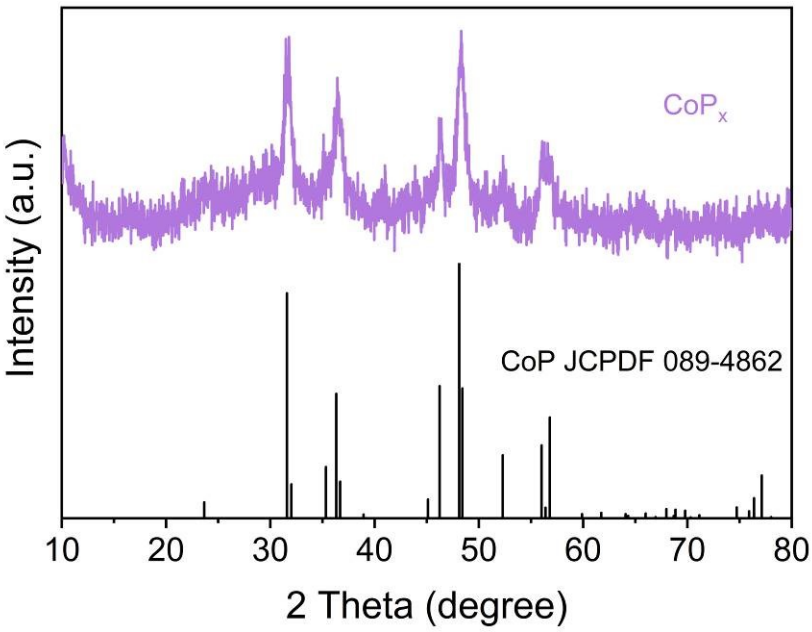

Fig. S6 XRD pattern of CoP_x material.

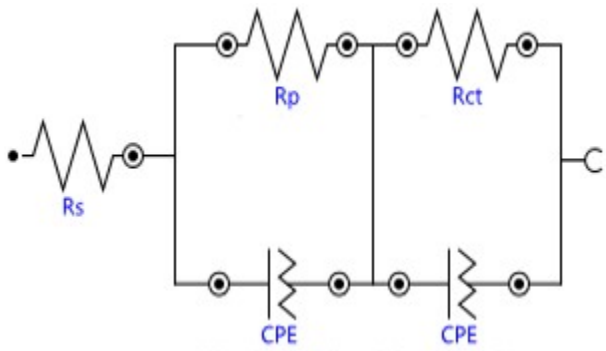

Fig. S7 Equivalent electrical circuit used to model the HER kinetics process. R_s is the solution resistance, CPE (on the left) and R_p are the element and resistance describing electron transport at catalyst interface, respectively. CPE (on the right) is the element of the catalyst/electrolyte interface, and R_{ct} is the charge transfer resistance at catalyst/electrolyte interface.[2]

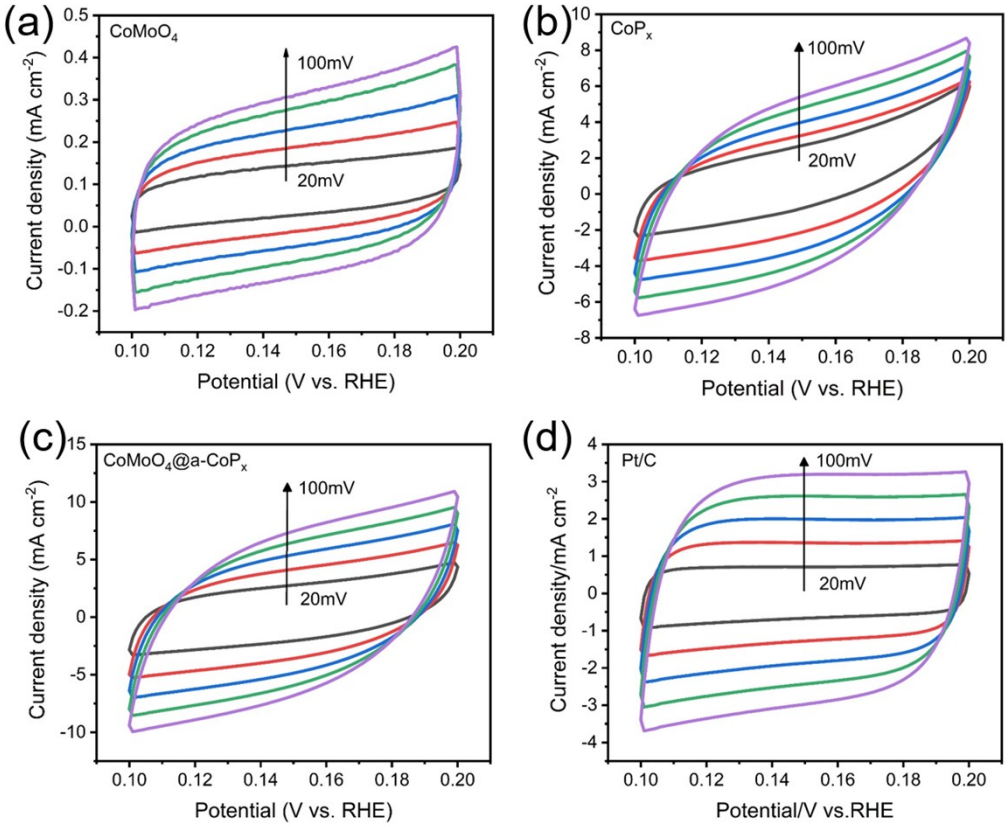

Fig. S8 Cyclic voltammograms curves of $CoMoO_4$ (a), a-CoP_x (b), $CoMoO_4$@a-CoP_x (c), and Pt/C (d).

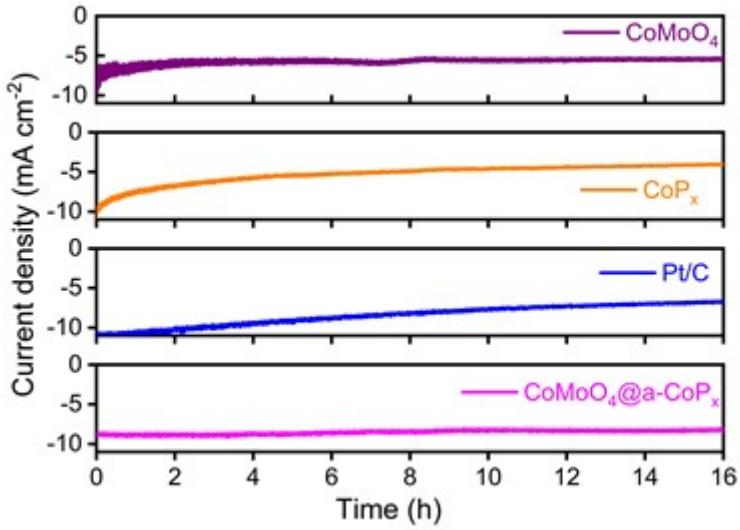

Fig. S9 Durability tests of $CoMoO_4$, CoP_x, $CoMoO_4$@a-CoP_x, and Pt/C.

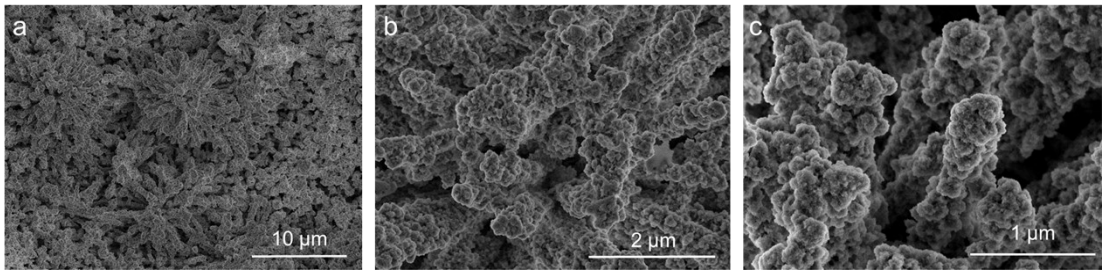

Fig. S10 (a-c) SEM images of $CoMoO_4$@a-CoP_x after the stability test.

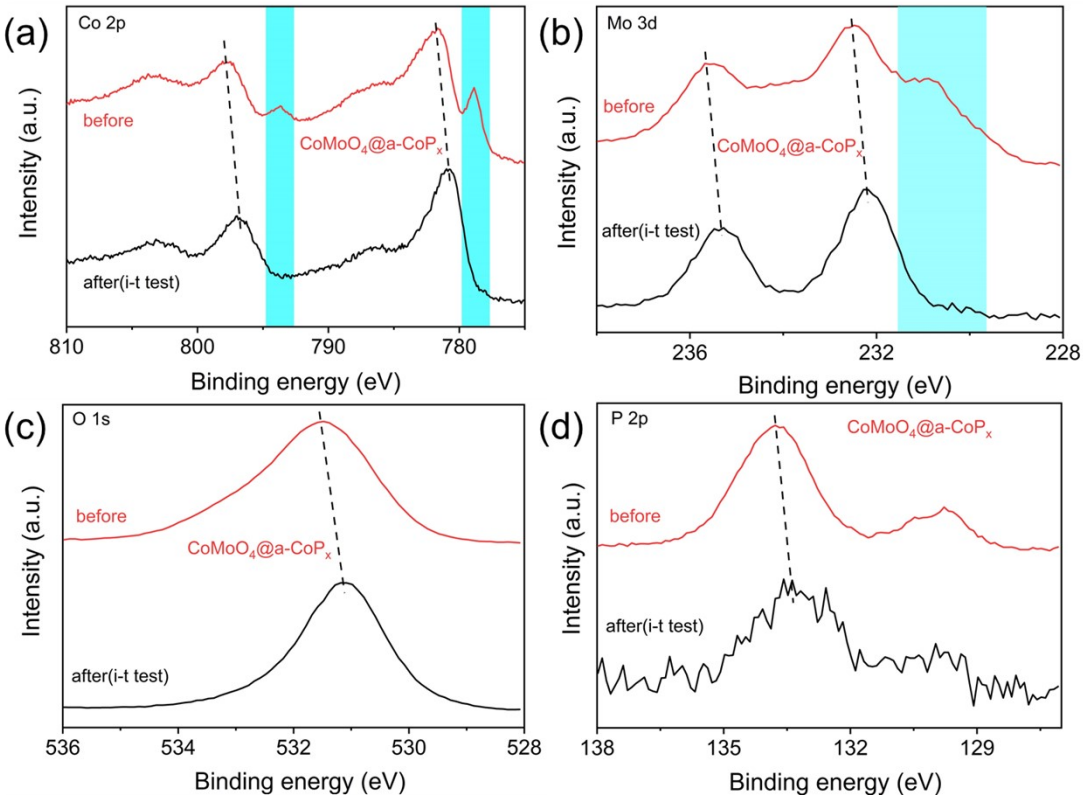

Fig. S11 (a) Co 2p, (b) Mo 3d, (c) O 1s and (d) P 2p XPS spectra of $CoMoO_4$@a-CoP_x samples before and after the stability test.

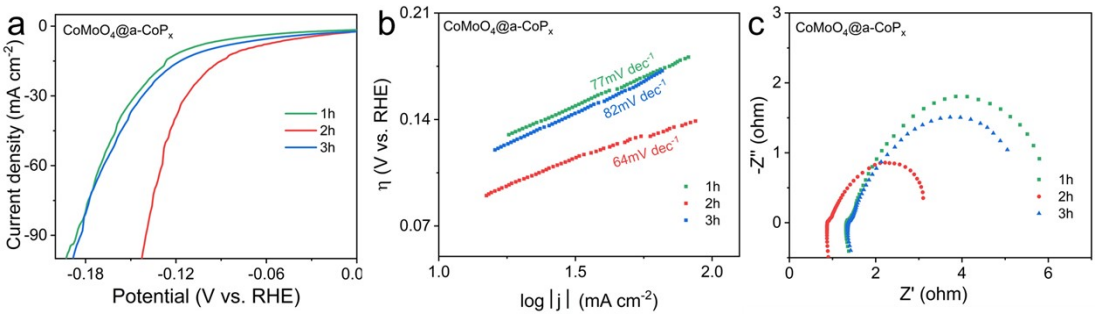

Fig. S12 (a) The HER iR-corrected polarization curves of $CoMoO_4$ with difference of the phosphating time at 300 °C as a scan rate of 2 mV • s^{-1} in 1 M KOH. (b) The corresponding Tafel plots. (c) Nyquist plots of the catalysts obtained at a potential of -0.1 V vs. RHE.

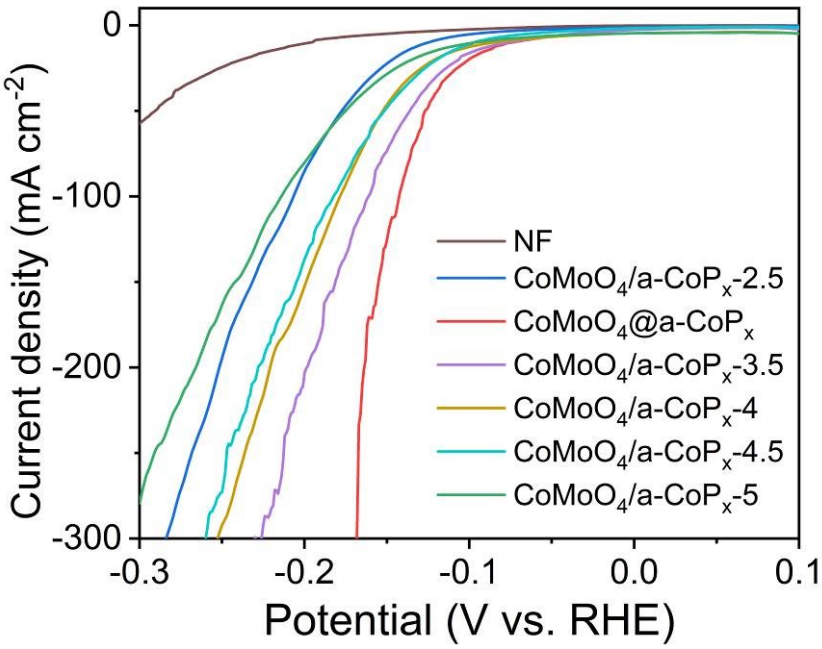

Fig. S13 The HER iR-corrected polarization curves of $CoMoO_4$ with different phosphating temperature in 1 M KOH.

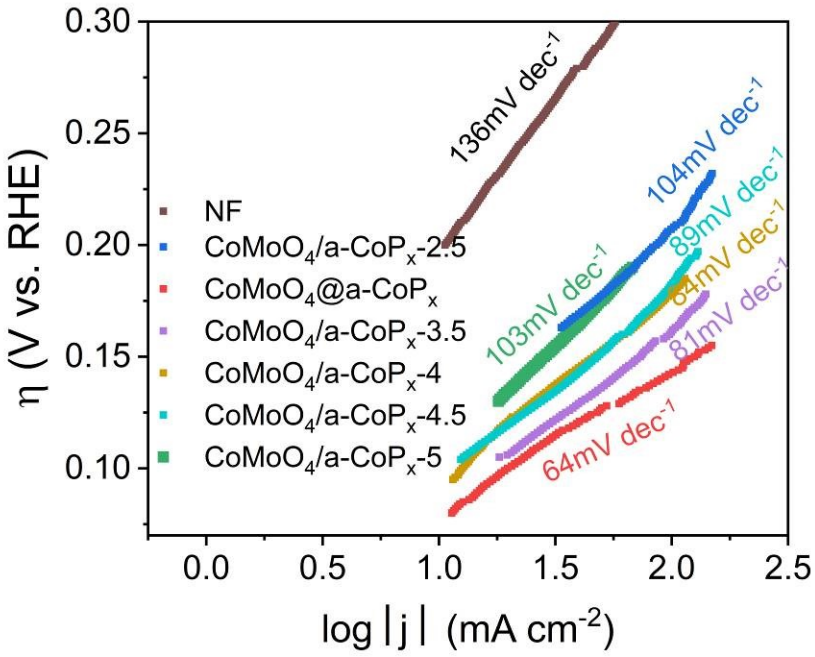

Fig. S14 Corresponding Tafel plots derived from Fig. S13.

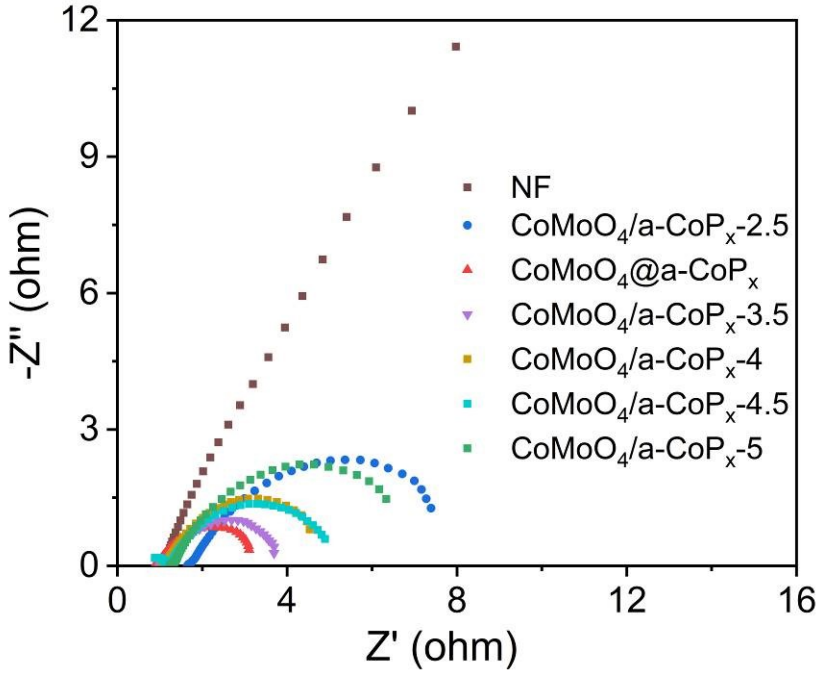

Fig. S15 EIS plots of $CoMoO_4$/a-CoP_x-x (x=2.5, 3, 3.5, 4, 4.5 and 5) with different phosphating temperature.

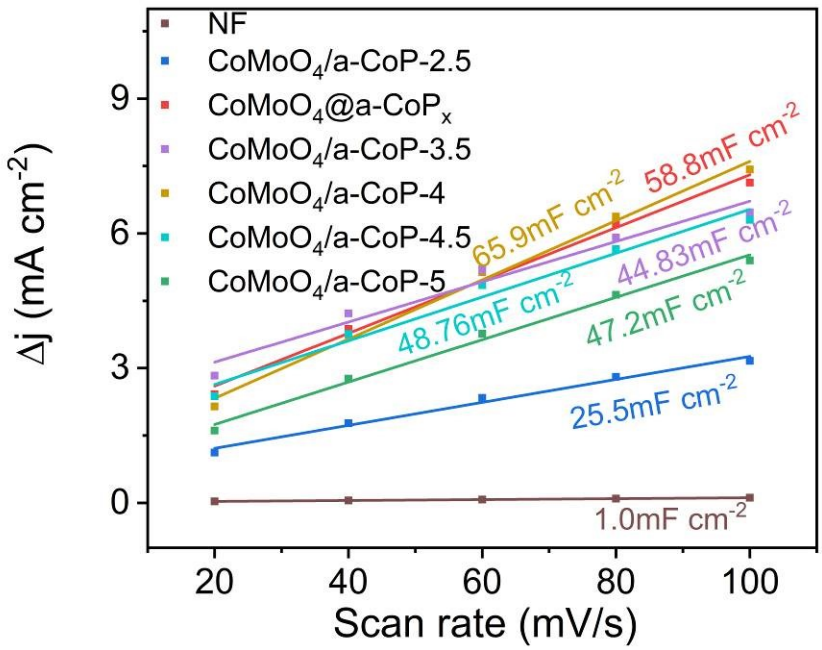

Fig. S16 The capacitive currents at 0.15 V vs. RHE as a function of scan rate for the corresponding catalysts in 1 M KOH solution.

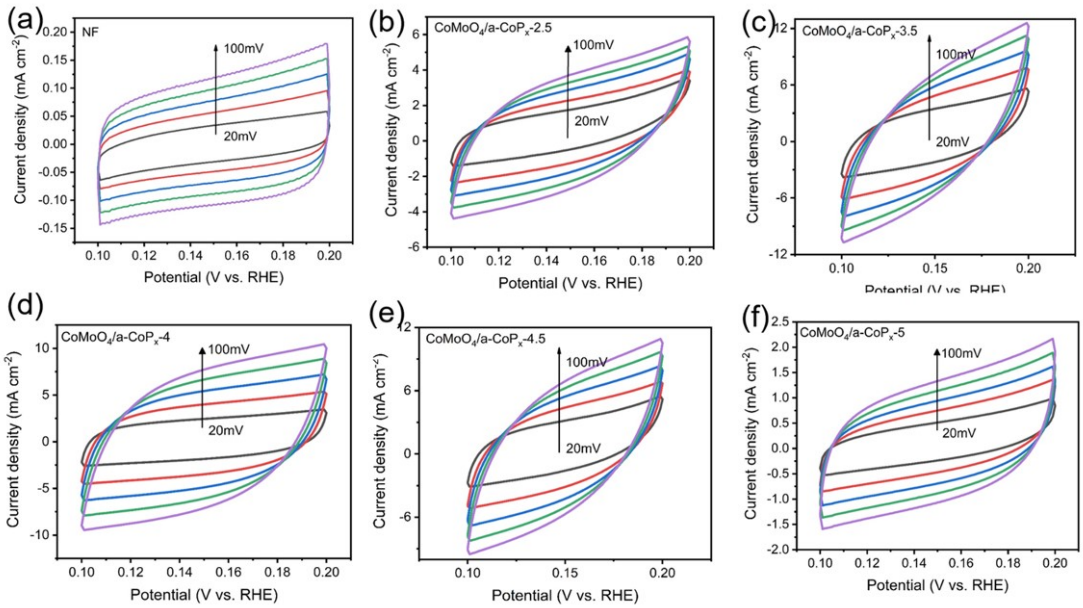

Fig. S17 Cyclic voltammograms curves of NF (a); $CoMoO_4$ electrodes after phosphating treatment at (b) 250 °C, (c) 350 °C, (d) 400 °C, (e) 450 °C and (f) 500 °C for 2h in region of 0.1~0.2 V vs. RHE at various scan rate. (f) The capacitive currents at 0.15 V vs RHE as a function of scan rate for the corresponding catalysts (1 M KOH solution).

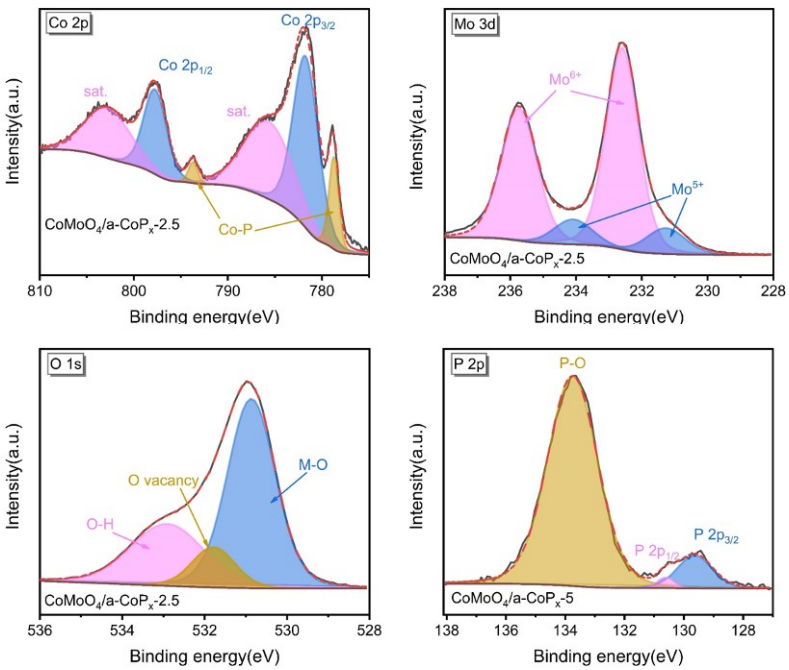

Fig. S18 XPS spectra [Co 2p, Mo 3d, O 1s, P 2p] of $CoMoO_4$/a-CoP_x-2.5.

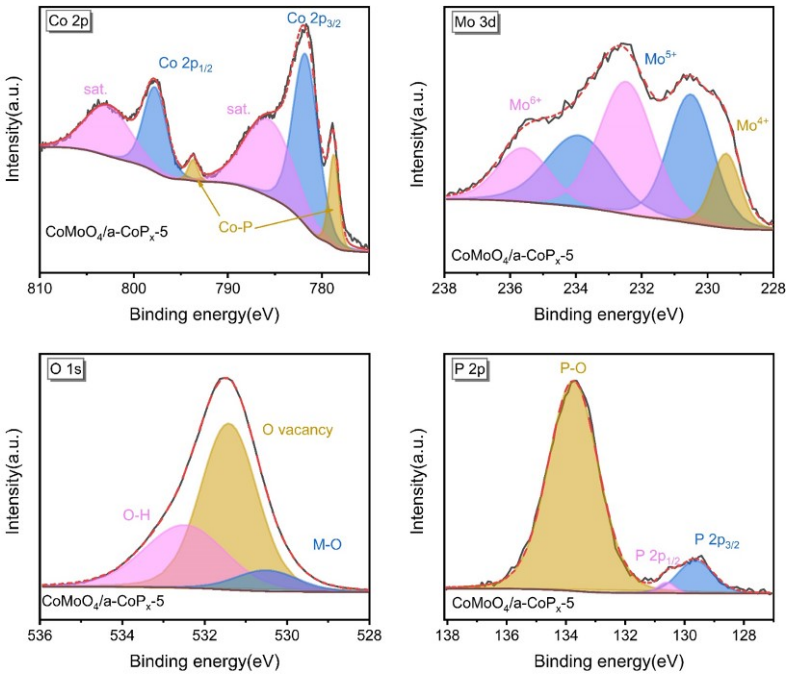

Fig. S19 XPS spectra [Co 2p, Mo 3d, O 1s, P 2p] of $CoMoO_4$/a-CoP_x-5.

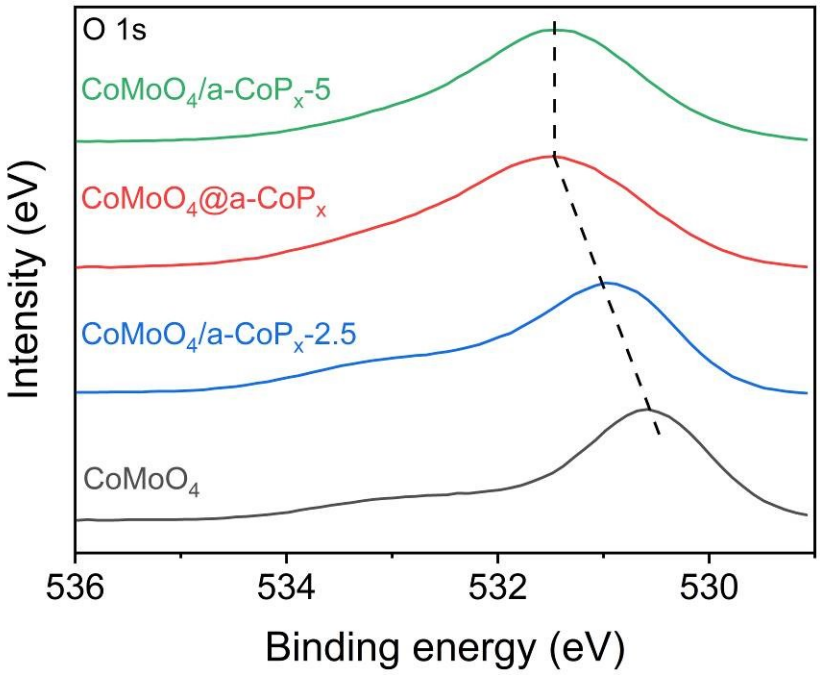

Fig. S20 XPS spectra O 1s of $CoMoO_4$, $CoMoO_4$/a-CoP_x-2.5, $CoMoO_4$@a-CoP_x and $CoMoO_4$/a-CoP_x-5.

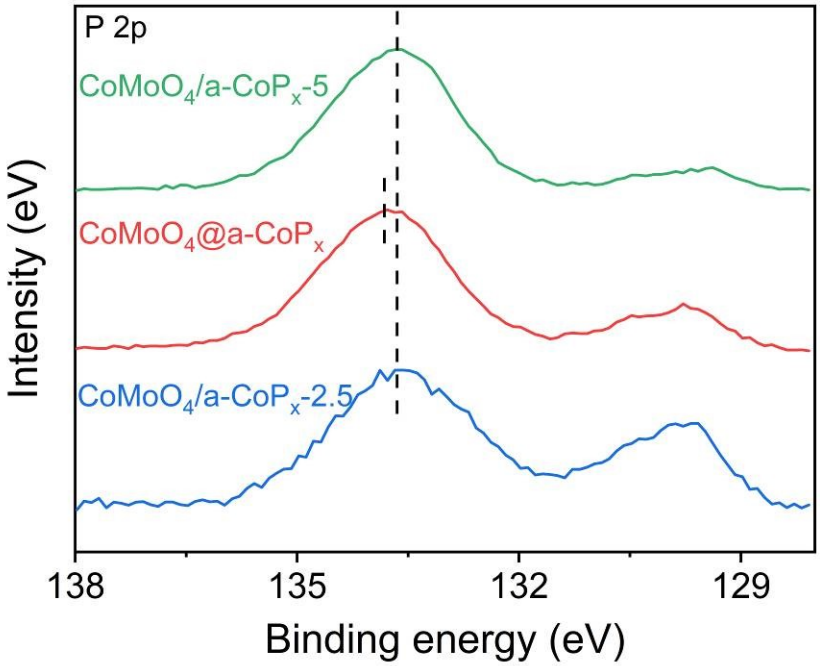

Fig. S21 XPS spectra P 2p of $CoMoO_4$/a-CoP_x-2.5, $CoMoO_4$@a-CoP_x and $CoMoO_4$/a-CoP_x-5.

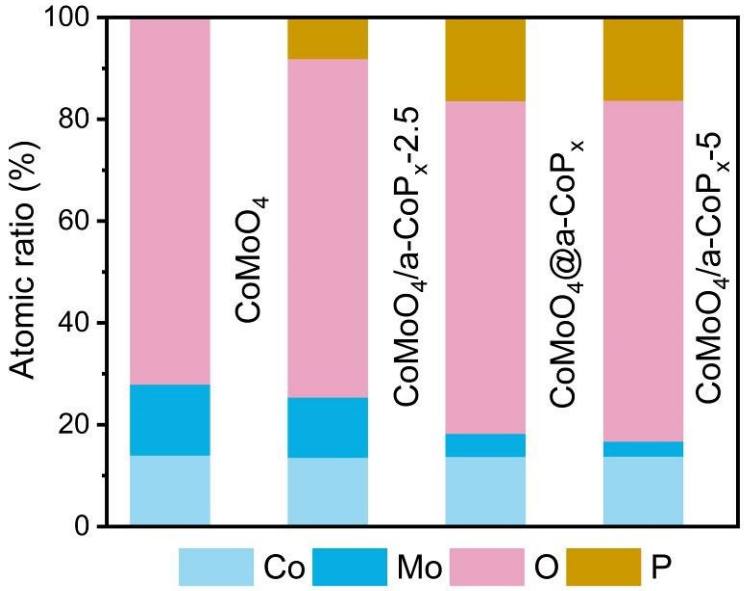

Fig. S22 Content diagram of elements in XPS before and after phosphating.

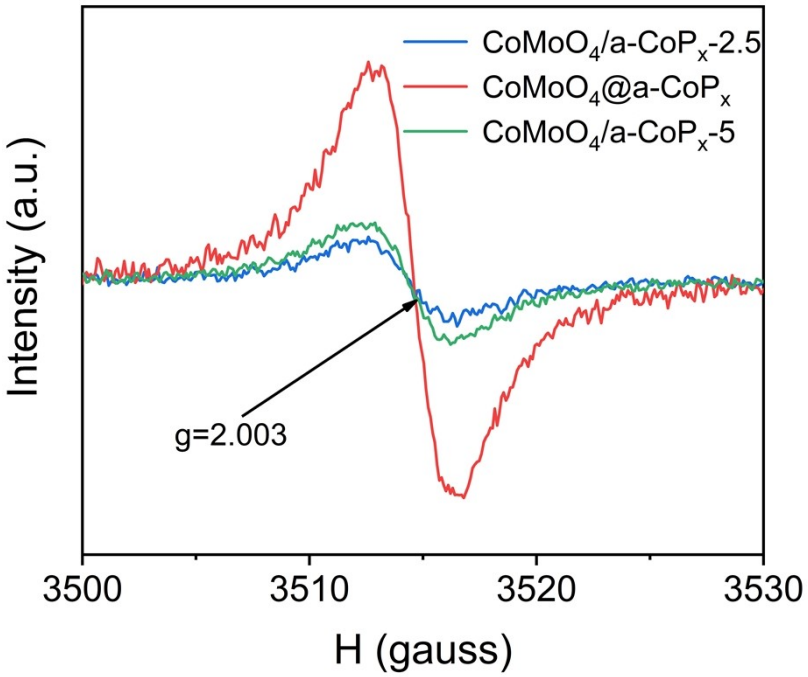

Fig. S23 EPR of $CoMoO_4$/a-CoP_x-2.5, $CoMoO_4$@a-CoP_x and $CoMoO_4$/a-CoP_x-5 samples.

Table S1 Activity comparison of $CoMoO_4$@a-CoP_x materials with other highly efficient transition metal-based catalysts at 1 M KOH for HER.

Catalysts	Overpotential(mV)		Tafel slope (mV/dec)	Reference
	j=10mA/cm^2	j=100mA/cm^2		
$CoMoO_4$@a-CoP_x/NF	74.7	144.3	64	This work
Ni2P–Ni12P5/NF	76	147	68	[3]
Mo-CoP/NC/TF	78		48.1	[4]
CoP/NPC/TF	80		50	[5]
CMP-350	94	197	93	[6]
Ni-doped FeP/C	95		72	[7]
N-NiMoO4/NiS2	99	-	74.2	[8]
Ni-SA/NC	102		120	[9]
S-Doped MoP	104		56	[10]
CoP/CN/Ni	106	-	64.6	[11]
CoP3/CoMoP-5/NF	110	-	64.1	[12]
CoP/NCNHP	115		66	[13]
NiCo2O4@CoMoO4/NF-7	121		77	[14]
CoP NFs	136	-	56.2	[15]
H-Fe-CoMoS	137	-	98	[16]
Amorphous CoP	143	-	63	[17]
CoP/NCNT-CP	165		96	[18]
CoPx@CNS	171	-	129	[19]
CoP/Ni2P	200	-	103	[20]
CNP-2	200		103	[21]
Co2P/CoNPC	208	-	83.9	[22]

Table S2 EIS data of $CoMoO_4$, a-CoP_x, $CoMoO_4$@a-CoP_x and Pt/C in HER tests.

Samples	R_s (Ω)	R_{ct} (Ω)
$CoMoO_4$	1.240	29.00
CoP_x	1.410	3.48
$CoMoO_4$@a-CoP_x	0.883	2.46
Pt/C	0.573	0.71

Table S3 Double layer capacitance (C_{dl}), calculated ECSA of the prepared materials over NF (C_s value is 1.7 mF cm^{-2}).

Samples	C_{dl} (mF)	ECSA (cm^2)
$CoMoO_4$	2.0	1.2
a-CoP_x	40.7	23.9
$CoMoO_4$/ a-CoP_x-2.5	25.5	15.0
$CoMoO_4$@a-CoP_x	58.8	34.6
$CoMoO_4$/ a-CoP_x-3.5	44.8	26.3
$CoMoO_4$/ a-CoP_x-4	65.9	38.6
$CoMoO_4$/ a-CoP_x-4.5	48.7	28.6
$CoMoO_4$/ a-CoP_x-5	47.2	27.7
Pt/C	29.9	17.6

Table S4 Elemental quantification results of $CoMoO_4$, $CoMoO_4$/a-CoP_x-2.5, $CoMoO_4$@a-CoP_x and $CoMoO_4$/a-CoP_x-5 through XPS analysis.

Atomic (%) / Samples	Co	Mo	O	P
CoMoO4	14.06	13.95	71.99	--
$CoMoO_4$/a-CoP_x-2.5	13.64	11.82	66.47	8.07
$CoMoO_4$@a-CoP_x	13.8	4.53	65.35	16.32
$CoMoO_4$/a-CoP_x-5	13.86	2.95	66.96	16.23

"--" indicate there is no this element in sample.

References:

[1] X. Huang, X. Xu, X. Luan, and D. Cheng, *Nano Energy,* 2019, **68**, 104332.

[2] Y. Lin, K. Sun, S. Liu, X. Chen, Y. Cheng, W. Cheong, Z. Chen, L. Zheng, J. Zhang, X. Li, *Adv. Energy Mater.,* 2019, **9**, 1901213.

[3] Z. Wang, S. Wang, L. Ma, Y. Guo, and R. Jiang, *Small,* 2021, **17**, 2006770.

[4] B. Yla, Z. C. Bao, B. Ww, A. Xs, Z. A. Jin, W. A. Rui, A. Bh, W. D. Qiang, C. Jj, A. Yg, *Chem. Eng. J.,* 2020, **405**, 126981.

[5] X. Huang, X. Xu, C. Li, D. Wu, D. Cheng, and D. Cao, *Adv. Energy Mater.,* 2019, **9**, 1803970.

[6] S. Zhao, J. Berry-Gair, W. Li, G. Guan, and I. P. Parkin, *Adv. Sci.,* 2020, **7**, 190374.

[7] X. F. Lu, L. Yu, and X. W. D. Lou, *Science Adv., 2019,* **5**, 6009.

[8] L. An, J. Feng, Y. Zhang, R. Wang, H. Liu, G. C. Wang, F. Cheng, P. Xi, *Adv. Funct. Mater.* 2019, **29**, 1805298.

[9] W. Zang, T. Sun, T. Yang, S. Xi, M. Waqar, Z. Kou, S. J. Pennycook, *Adv. Mater.,* 2021, **33**, 2003846.

[10] K. Liang, S. Pakhira, Z. Yang, A. Nijamudheen, and Y. Yang, *ACS Catalysis,* 2018, **9**, 651-659.

[11] C. Teng, B. Jm, A. Sc, B. Yw, A. Cd, A. Jc, B. Jh, A. Wd, *Chem. Eng. J.,* 2021, **415**, 129031.

[12] D. Jiang, Y. Xu, R. Yang, D. Li, S. Meng, and M. Chen, *ACS Sustainable Chem. Eng.,* 2019, **7**, 9309-9317.

[13] Y. Pan, K. Sun, S. Liu, X. Cao, K. Wu, W.C. Cheong, Z. Chen, Y. Wang, Y. Li, Y. Liu, *J. Am. Chem. Soc.,* 2018, **140**, 210-2618.

[14] Y. Gong, Z. Yang, Y. Lin, J. Wang, H. Pan, Z. Xu, *J. Mater. Chem. A,* 2018, **6**, 16950-16958.

[15] L. Ji, J. Wang, X. Teng, T. J. Meyer, Z. Chen, *ACS Catalysis,* 2019, **10**, 412-419.

[16] Y. Guo, X. Zhou, J. Tang, S. Tanaka, and Y. Sugahara, *Nano Energy,* 2020, **75**, 104913.

[17] M. Driess, R. B. Suito, and P. M. Menezes, *J. Mater. Chem. A,* 2019, **7**, 15749-15756.

[18] L. Wang, J. Cao, X. Cheng, C. Lei, Q. Dai, B. Yang, Z. Li, M. A. Younis, L. Lei, Y. Hou, *ACS Sustainable Chem. Eng.,* 2019, **7**, 10044-10051.

[19] C. Hou, L. Zou, Y. Wang, and Q. Xu, *Angew. Chem., Int. Ed.,* 2020, **132**, 21544-21550.

[20] J. Zhang, S. Wei, Y. Liu, G. Wang, Y. Cui, A. Dong, S. Xu, J. Lian, Q. Jiang, *J. Mater. Chem. A,* 2019, **7**, 26177-26186.

[21] Y. Gong, Z. Yang, Y. Lin, J. Wang, H. Pan, Z. Xu, *J. Mater. Chem. A,* 2018, **6**, 16950-16958.

[22] H. Liu, J. Guan, S. Yang, Y. Yu, and Q. Xu, *Adv. Mater.,* 2020, **32**, 2003469.